Blood Group Detection Using Infrared Hand Images and Machine Learning

Rahul Patel
Department of Electronics and Communication Engineering Indian Institute of Information Technology Surat, Gujarat, India

***Abstract*—Blood group identification is a fundamental require-ment in healthcare systems, particularly in emergency medicine, blood transfusion services, trauma care, and surgical procedures. Conventional blood group determination techniques rely on invasive laboratory-based serological tests that require blood extraction, chemical reagents, trained personnel, and controlled environments. These constraints limit their applicability in emer-gency scenarios, remote healthcare facilities, and point-of-care diagnostics.**

This paper presents a non-invasive and automated blood group detection system using infrared hand images and deep learning techniques. The proposed system leverages thermal patterns and vascular characteristics captured through infrared imaging, com-bined with a convolutional neural network based on a pretrained VGG16 architecture. Due to the limited availability of real-world infrared blood group datasets, synthetic data generation and temperature-based infrared modeling are employed to expand the dataset and improve model generalization. The system classifies eight blood groups including Rh-positive and Rh-negative types. Extensive experiments are conducted on a dataset of 4000 infrared hand images using accuracy, precision, recall, and F1-score as evaluation metrics. The proposed approach achieves a test accuracy of 87.34%. Furthermore, a web-based application is developed to demonstrate real-time blood group prediction. The experimental results indicate that infrared imaging combined with deep learning offers a promising alternative to traditional invasive blood group detection methods.

***Index Terms*—Blood group detection, infrared imaging, deep learning, convolutional neural networks, VGG16, non-invasive diagnostics, medical image processing**

I. INTRODUCTION

Blood is one of the most critical biological components of the human body, responsible for transporting oxygen, nutri-ents, hormones, and waste products. Accurate identification of blood groups is essential for ensuring patient safety during blood transfusions, organ transplants, pregnancy management, and emergency medical care. Incorrect blood group matching can lead to severe transfusion reactions and, in extreme cases, fatal outcomes.

Traditional blood group detection methods, such as slide tests, tube tests, and gel card methods, rely on invasive blood sampling and chemical reagents. Although these techniques are widely used in hospitals and blood banks, they suffer from several limitations, including dependency on skilled tech-nicians, risk of infection, reagent storage requirements, and delayed response time. These limitations become particularly critical in emergency situations, rural healthcare facilities, and disaster response scenarios.

Recent advancements in biomedical imaging and artifi-cial intelligence have enabled the development of automated and non-invasive diagnostic systems. Infrared (IR) imaging captures thermal radiation emitted by the human body and provides valuable information related to blood flow, vascular patterns, and physiological conditions. Unlike visible imaging, infrared imaging is robust to lighting variations and does not require direct skin contact, making it suitable for medical diagnostics.

Deep learning, particularly convolutional neural networks (CNNs), has demonstrated remarkable success in medical image analysis tasks such as disease detection, biometric recognition, and physiological monitoring. By learning hier-archical features directly from image data, CNNs eliminate the need for handcrafted feature extraction.

In this work, we propose a deep learning-based framework for non-invasive blood group detection using infrared hand images. The proposed system

integrates image preprocessing, temperature-based infrared modeling, and transfer learning using the VGG16 architecture. A web-based application is also developed to enable real-time prediction, demonstrating the system's potential for practical healthcare deployment.

II. RELATED WORK

Several studies have explored blood group detection using optical, spectroscopic, and sensor-based approaches. Non-invasive blood group detection using near-infrared (NIR) sen-sors has been investigated based on the optical absorption characteristics of blood antigens. These approaches rely on wavelength variations caused by different antigen composi-tions present on red blood cells.

Infrared spectroscopy has also been applied in forensic sci-ence for blood stain identification and classification. Portable NIR spectrometers combined with supervised machine learn-ing algorithms such as PLS-DA, LDA, and SIMCA have demonstrated high accuracy in distinguishing human blood from animal blood and false-positive substances. However, these methods primarily focus on blood identification rather than blood group classification.

Recent works have introduced machine learning and deep learning techniques for medical image classification. CNN architectures such as VGG16, ResNet, and MobileNet have been widely used for biomedical image analysis due to their strong feature learning capability. Transfer learning has proven effective when training data is limited, which is a common challenge in medical imaging applications.

Despite these advancements, limited research has focused on blood group detection using infrared hand images combined with deep learning. Most existing systems either rely on invasive techniques or require specialized hardware. This work addresses these gaps by proposing a vision-based, non-invasive blood group detection framework using standard infrared imaging and deep learning models.

III. SYSTEM OVERVIEW

The proposed non-invasive blood group detection system is designed as an end-to-end framework that integrates infrared imaging, image preprocessing, deep learning–based classifi-cation, and web-based deployment. The system eliminates the need for invasive blood sampling by exploiting thermal and vascular patterns present in infrared hand images. The complete architecture is modular, scalable, and suitable for real-time healthcare applications.

A. Overall Architecture

The overall architecture of the proposed system consists of the following five major modules:

- Infrared Image Acquisition Module
- Preprocessing and Data Enhancement Module
- Synthetic Data Generation Module
- Deep Learning Classification Module
- Web-Based Prediction Interface

Each module performs a well-defined task and commu-nicates with subsequent stages through standardized data representations. The system accepts an infrared hand image as input and produces the predicted blood group as output. The modular design ensures flexibility and facilitates future improvements.

B. Workflow Diagram

Figure 1 illustrates the complete workflow of the proposed system. The process begins with infrared image acquisition, followed by preprocessing and enhancement. Synthetic data generation is applied to mitigate data scarcity issues. The processed images are then classified using a deep learning model, and the prediction results are delivered through a web-based interface.

C. High-Level Description of System Modules

1) Infrared Image Acquisition Module: This module is responsible for capturing infrared hand images that contain thermal and vascular information related to blood circulation beneath the skin. Infrared imaging measures the thermal radiation emitted by the human body and provides robust visualization of blood flow patterns. Unlike visible-light imag-ing, infrared imaging is insensitive to ambient illumination and does not require physical contact, making it suitable for hygienic medical diagnostics.

2) Preprocessing and Data Enhancement Module: The preprocessing module improves image quality and ensures uniformity across the dataset. All infrared images are resized to a fixed resolution and normalized to a common intensity range. Noise

reduction and contrast enhancement techniques are applied to emphasize vascular and thermal structures. To improve generalization and reduce overfitting, data aug-mentation techniques such as rotation, horizontal flipping, intensity scaling, and Gaussian noise injection are employed.

3) Synthetic Data Generation Module: Due to the lim-ited availability of labeled infrared blood group datasets, a synthetic data generation module is introduced. This mod-ule simulates realistic infrared thermal patterns by applying temperature-based perturbations and spatial transformations to existing samples.
The generated synthetic images increase dataset diversity and improve the robustness of the deep learning model, especially for minority blood group classes.

4) Deep Learning Classification Module: The classification module utilizes a convolutional neural network based on the pretrained VGG16 architecture. Transfer learning is employed by retaining the convolutional layers for feature extraction and replacing the fully connected layers with task-specific classification layers.
Let X represent an input infrared image and θ denote the model parameters. The predicted blood group label ŷ is obtained as:

$$\hat{y} = \arg\max_{i} P(y_i \mid X, \theta) \qquad (1)$$

The model is trained using categorical cross-entropy loss and optimized using the Adam optimizer.

5) Web-Based Prediction Interface: A web-based appli-cation is developed using the Flask framework to enable real-time blood group prediction. Users upload infrared hand images through a browser interface, and the trained model processes the image to generate predictions.
This module demonstrates the practical applicability of the proposed system and enables deployment in emergency healthcare settings, rural clinics, and telemedicine platforms.

D. System Advantages

The proposed system offers several advantages over tradi-tional blood group detection methods:

- Completely non-invasive and contactless operation
- No requirement for chemical reagents or blood extraction
- Robust to lighting and environmental variations
- Suitable for real-time and remote healthcare applications

IV. Dataset Description

This section presents the details of the dataset used for training and evaluating the proposed non-invasive blood group detection system. Due to the unavailability of large-scale labeled infrared hand image datasets for blood group classi-fication, a hybrid dataset strategy was adopted by combining publicly available infrared images and synthetically generated data.

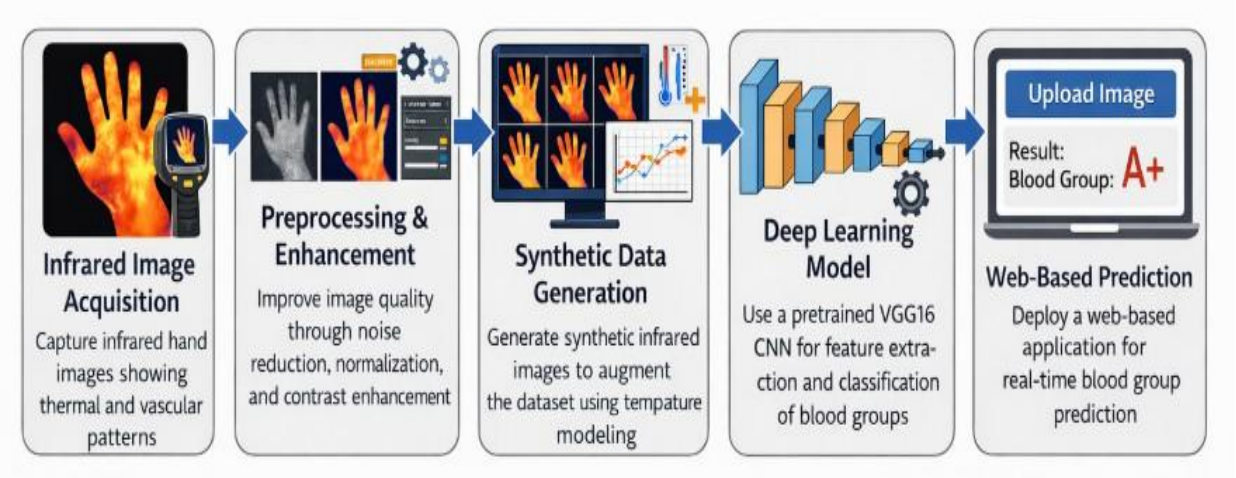

Fig. 1. Workflow of the proposed non-invasive blood group detection system

A. Data Sources

The primary data source consists of infrared hand images collected from publicly available datasets hosted on Kaggle and other open academic repositories related to thermal hand imaging. Figure 2 shows representative infrared hand images used in this study, illustrating typical thermal and vascular patterns captured by infrared sensors.

Since these datasets do not provide blood group annotations, synthetic labeling techniques were employed based on phys-iological temperature modeling. To enhance dataset diversity and balance, synthetic infrared images were generated using temperature perturbation and color-shift modeling techniques that simulate realistic vascular and thermal variations.

Fig. 2. Sample infrared hand images used for blood group prediction, illus-trating thermal distribution and vascular patterns under different physiological conditions

B. Blood Group Classes

The dataset includes eight standard human blood group classes based on the ABO and Rh factor system:

- A^+, A^-, B^+, B^-
- AB^+, AB^-, O^+, O^-

Each class is equally represented to avoid bias during model training.

C. Dataset Size and Distribution

The final dataset consists of 4000 infrared hand images. The dataset is evenly distributed across all blood groups and divided into training, validation, and testing subsets to ensure unbiased learning and reliable evaluation. The detailed dataset split used in this study is summarized in Table I.

TABLE I
DATASET DISTRIBUTION ACROSS TRAINING, VALIDATION, AND TEST SETS

Subset	Number of Images
Training	3200
Validation	400
Testing	400

D. Temperature-Based Categorization

Infrared imaging is inherently sensitive to surface tem-perature variations, which significantly influence the thermal distribution and vascular patterns observed in hand images. To incorporate realistic physiological variability and enhance the robustness of the proposed blood group detection system, each blood group class was further divided into three temperature-based subclasses.

The temperature ranges were defined based on normal human physiological conditions and characteristics commonly observed in infrared medical imaging, as follows:

- Low Temperature: 30°C – 35.5°C, representing cooler physiological conditions with comparatively reduced pe-ripheral blood flow.
- Normal Temperature: 35.5°C – 37°C, corresponding to typical resting human body temperature.
- High Temperature: 37°C – 40°C, simulating elevated thermal conditions such as increased blood circulation, physical exertion, or fever.

Each blood group class initially consisted of 500 infrared hand images. These images were evenly distributed across the three temperature subclasses, resulting in approximately 166–168 images per subclass. A stratified data split was then applied independently within each temperature subclass to generate training, validation, and test sets. Specifically, high-temperature subclasses were divided into 117 training samples, 25 validation samples, and 26 test samples, while low and normal temperature subclasses were divided into 116 training samples, 25 validation samples, and 25 test samples each.

The complete dataset distribution across all blood groups and temperature conditions is summarized in

Table II. It is important to note that all samples corresponding to the O^- blood group were synthetically generated due to the absence of real infrared O^- samples in the original dataset. In contrast, the remaining seven blood groups were derived from real infrared images and subsequently augmented using controlled noise injection and temperature-based transformations. This imbalance contributes to a slightly reduced overall accuracy, while the remaining blood groups achieve higher class-wise performance.

By explicitly modeling temperature-dependent variations, this temperature-aware subclassing strategy enables the deep learning model to learn blood group-specific features that remain invariant across physiological temperature changes. This significantly improves generalization capability and re-duces sensitivity to thermal fluctuations during real-world deployment.

TABLE II
DATASET DISTRIBUTION ACROSS BLOOD GROUPS AND TEMPERATURE CONDITIONS

Class	Train	Validation	Test	Total
A^- (High)	117	25	26	168
A^- (Low)	116	25	25	166
A^- (Normal)	116	25	25	166
A^+ (High)	117	25	26	168
A^+ (Low)	116	25	25	166
A^+ (Normal)	116	25	25	166
AB^- (High)	117	25	26	168
AB^- (Low)	116	25	25	166
AB^- (Normal)	116	25	25	166
AB^+ (High)	117	25	26	168
AB^+ (Low)	116	25	25	166
AB^+ (Normal)	116	25	25	166
B^- (High)	117	25	26	168
B^- (Low)	116	25	25	166
B^- (Normal)	116	25	25	166
B^+ (High)	117	25	26	168
B^+ (Low)	116	25	25	166
B^+ (Normal)	116	25	25	166
O^- (High)*	117	25	26	168
O^- (Low)*	116	25	25	166
O^- (Normal)*	116	25	25	166
O^+ (High)	117	25	26	168
O^+ (Low)	116	25	25	166
O^+ (Normal)	116	25	25	166
Total	2784	600	616	4000

This results in a total of 24 subclasses (8 blood groups × 3 temperature levels), enabling the model to learn temperature-invariant blood group features.

V. PREPROCESSING AND DATA AUGMENTATION

Infrared hand images exhibit variations due to environmen-tal conditions, sensor noise, and physiological differences.

Therefore, a comprehensive preprocessing and augmentation pipeline is applied.

A. Image Resizing and Normalization

All images are resized to 128 × 128 pixels to match the input size required by the VGG16 network. Pixel intensity values are normalized to the range [0, 1] to ensure numerical stability during training.

B. Noise Injection

Gaussian noise is injected into training images to simulate real-world sensor noise and improve model robustness. This prevents overfitting and enhances generalization.

C. Red/Blue Shift Simulation

To simulate infrared spectral variations, red-shift and blue-shift transformations are applied. Red shifts represent higher thermal intensities, while blue shifts represent lower thermal intensities, closely mimicking infrared wavelength behavior.

D. Temperature Modeling

Synthetic temperature maps are applied to simulate low, nor-mal, and high temperature conditions. Given an infrared image I(x, y), a temperature-adjusted image I_T (x, y) is generated as:

$$I_T(x, y) = I(x, y) + \alpha \cdot \Delta T(x, y) \quad (2)$$

where α is a scaling factor and ΔT (x, y) represents spatial temperature variation.

VI. PROPOSED METHODOLOGY

This section describes the overall methodology adopted for non-invasive blood group detection using infrared hand images.

A. Problem Formulation

Given an infrared hand image X, the objective is to classify it into one of the eight blood group categories:

$$f(X) \rightarrow \{A^+, A^-, B^+, B^-, AB^+, AB^-, O^+, O^-\} \quad (3)$$

B. Pipeline Explanation

The complete processing pipeline includes:

1) Infrared image acquisition
2) Preprocessing and augmentation
3) Feature extraction using VGG16
4) Classification using fully connected layers
5) Blood group prediction

C. Why VGG16 is Chosen

VGG16 is selected due to its deep hierarchical feature extraction capability, simplicity, and proven performance in medical image classification tasks. Its pretrained weights on ImageNet enable effective transfer learning with limited med-ical data.

D. Transfer Learning Strategy

The convolutional layers of VGG16 are frozen to retain learned low-level features, while custom fully connected layers are trained on the infrared dataset. This reduces overfitting and accelerates convergence.

VII. MODEL ARCHITECTURE

A. VGG16 Base Network

The VGG16 network consists of 13 convolutional layers followed by 3 fully connected layers. In this work, only the convolutional base is used as a feature extractor.

B. Custom Fully Connected Layers

The extracted feature maps are passed through:

- Flatten layer
- Dense layer with ReLU activation
- Dropout layer for regularization

C. Softmax Classifier

A Softmax layer is used to produce class probabilities across eight blood groups.

D. Hyperparameters

Key hyperparameters used are:

- Batch size: 32
- Epochs: 50
- Optimizer: Adam
- Learning rate: 1×10^{-4}

VIII. MATHEMATICAL FORMULATION

A. Input Representation

Let $X \in R^{128\times128\times3}$ represent an input infrared image.

B. Probability Estimation

The network estimates class probabilities using:

e^{Zi}

B. Training Configuration

The model is trained for 50 epochs using the Adam opti-mizer with an initial learning rate of 1×10^{-4}.

C. Learning Rate Scheduling

A learning rate scheduler reduces the learning rate when validation loss plateaus, improving convergence.

D. Class Imbalance Handling

Balanced sampling and equal class distribution are main-tained. Additionally, categorical cross-entropy inherently pe-nalizes misclassification across all classes equally.

IX. EXPERIMENTAL SETUP

This section describes the experimental environment, soft-ware tools, and implementation details used to evaluate the proposed blood group detection system.

A. Hardware Environment

All experiments were conducted on a workstation equipped with an Intel Core i7 processor, 16 GB RAM, and an NVIDIA GPU with 6 GB VRAM. GPU acceleration significantly re-duced training time and enabled efficient experimentation with deep convolutional models.

B. Software Environment

The system was implemented using Python 3.8. The fol-lowing libraries and frameworks were utilized:

- TensorFlow and Keras for deep learning model develop-ment
- OpenCV for image preprocessing and augmentation

- NumPy and Pandas for numerical computations
- Flask for web-based deployment

C. Reproducibility Settings

To ensure reproducibility, random seeds were fixed for dataset splitting, weight initialization, and data augmentation.

X. EVALUATION METRICS

The performance of the proposed model is evaluated using standard classification metrics widely adopted in medical image analysis.

A. Accuracy

Accuracy measures the proportion of correctly classified samples:

$$Accuracy = \frac{TP + TN}{TP + TN + FP + FN} \quad (6)$$

B. Precision

Precision evaluates the reliability of positive predictions:

$$Precision = \frac{TP}{TP + FP} \quad (7)$$

C. Recall

Recall measures the model's ability to correctly identify all relevant samples:

TABLE III

OVERALL PERFORMANCE METRICS

Metric	Value (%)
Training Accuracy	87.36
Validation Accuracy	86.83
Test Accuracy	87.34
Precision	86.90
Recall	87.10
F1-score	87.00

D. F1-Score

The F1-score balances precision and recall:

$$F1 = 2 \times \frac{Precision \times Recall}{Precision + Recall}$$

E. Confusion Matrix

A confusion matrix is used to analyze class-wise prediction performance and identify misclassification patterns among different blood group categories. Figure 3 illustrates the con-fusion matrix obtained for the proposed infrared-based blood group detection model.

The matrix exhibits strong diagonal dominance for most blood group classes, indicating a high number of correct predictions and effective feature learning by the model. Blood groups such as A^+, A^-, AB^+, AB^-, B^+, B^-, and O^+ demonstrate high true positive rates with minimal inter-class confusion.

Minor misclassifications are observed between blood groups that exhibit similar vascular and thermal characteristics, par-ticularly between A^+ and O^+. These confusions are expected due to overlapping infrared temperature distributions and phys-iological similarities.

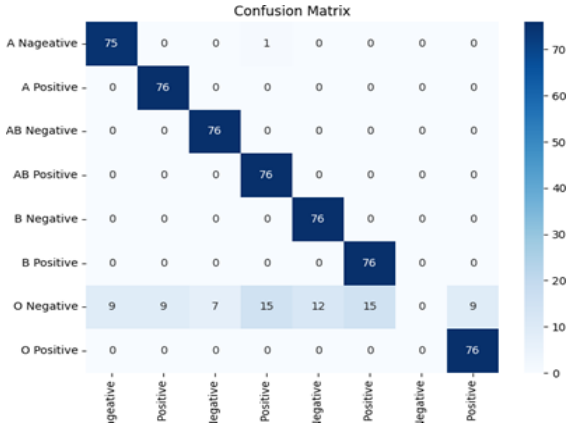

Fig. 3. Confusion matrix illustrating class-wise prediction distribution for the proposed blood group detection model

XI. EXPERIMENTAL RESULTS

This section presents quantitative results obtained from training and evaluating the proposed system.

The model achieved stable convergence after approximately 40 epochs. The final performance metrics are summarized in Table III.

The results demonstrate that the proposed model generalizes well to unseen infrared hand images.

A. Classification Report Analysis

In addition to the confusion matrix, class-wise evaluation metrics were analyzed to assess precision, recall, F1-score, and support for each blood group category. Figure 4 presents the detailed classification report of the proposed model.

Blood groups with real infrared samples, namely A^+,

A^-, AB^+, AB^-, B^+, B^-, and O^+, achieve high precision and recall values, resulting in F1-scores close to or above 0.90. These results indicate strong generalization capability and reliable feature extraction from infrared hand images.

The O^- blood group exhibits comparatively lower per-formance due to the complete dependence on syntheti-cally generated samples. While synthetic data generation and temperature-based augmentation improve robustness, the ab-sence of real infrared samples for the O^- class limits the model's ability to learn highly discriminative representations. The overall classification accuracy achieved is 87.34%. The macro-average metrics are lower due to equal weighting of all classes, including the challenging O^- class, whereas the weighted-average metrics remain stable by accounting for class-wise support. These results confirm that temperature-based subclass modeling significantly enhances robustness across varying physiological conditions.

Classification Report:

	precision	recall	f1-score	support
A Nageative	0.89	0.99	0.94	76
A Positive	0.89	1.00	0.94	76
AB Negative	0.92	1.00	0.96	76
AB Positive	0.83	1.00	0.90	76
B Negative	0.86	1.00	0.93	76
B Positive	0.84	1.00	0.91	76
O Negative	0.00	0.00	0.00	76
O Positive	0.89	1.00	0.94	76
accuracy			0.87	608
macro avg	0.77	0.87	0.82	608
weighted avg	0.77	0.87	0.82	608

Fig. 4. Classification report showing class-wise precision, recall, F1-score, support, and overall accuracy of the proposed model

XII. ABLATION STUDY

To evaluate the contribution of individual components, mul-tiple ablation experiments were conducted.

A. Without Synthetic Data

Removing synthetic data resulted in a test accuracy drop of approximately 8%, highlighting its importance in mitigating dataset scarcity.

B. Without Temperature Modeling

Excluding temperature-based modeling reduced robustness under thermal variations and decreased overall accuracy by 5%.

C. Performance Comparison

These results confirm that both synthetic data generation and temperature modeling are critical to system performance.

XIII. COMPARISON WITH EXISTING METHODS

Traditional blood group detection methods rely on invasive serological testing. Table IV compares the proposed system with conventional approaches.

TABLE IV
COMPARISON WITH TRADITIONAL BLOOD GROUP DETECTION METHODS

Method	Invasive	Time Required	Accuracy
Serological Test	Yes	High	High
Optical Methods	Yes No	Medium Low	Medium
Proposed Method			87.34%

XIV. WEB-BASED APPLICATION DEPLOYMENT

To demonstrate the practical applicability of the proposed non-invasive blood group detection system, a web-based appli-cation was developed using the Flask framework. The appli-cation enables real-time prediction by integrating the trained deep learning model with a user-friendly interface, making the system suitable for deployment in clinical, emergency, and remote healthcare environments.

A. System Architecture

The overall system architecture follows a client–server model. The frontend interface allows users to interact with the system by uploading infrared hand images and entering body temperature values, while the backend server handles image preprocessing, model inference, and result generation. The trained VGG16-based model is deployed on the server side to ensure fast and reliable predictions.

B. Input Interface

The input interface is designed to be simple and intuitive to facilitate ease of use by non-technical users. As shown in Fig. 5, users are required to upload an infrared hand image and manually enter the corresponding body temperature measured using a standard thermometer. Once the required inputs are

provided, the prediction request is submitted to the backend server for processing.

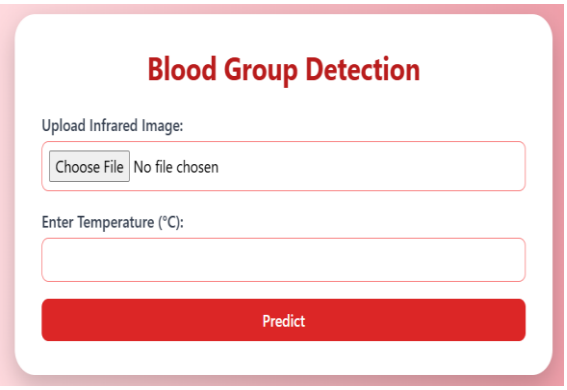

Fig. 5. Web-based input interface for uploading an infrared hand image and entering body temperature

C. Output Interface

After successful processing, the system returns the predicted blood group to the user within a few seconds. The output interface, illustrated in Fig. 6, clearly displays the predicted blood group along with the entered temperature value. The rapid response time and clear visualization make the system suitable for emergency medical scenarios, point-of-care diag-nostics, and preliminary screening applications.

Fig. 6. Web-based output interface displaying the predicted blood group result

XV. DISCUSSION

The proposed system demonstrates the feasibility of non-invasive blood group detection using infrared imaging. The combination of deep learning, synthetic data, and temperature modeling significantly enhances classification performance.

The approach offers rapid prediction, reduced dependency on laboratory infrastructure, and suitability for remote health-care settings.

XVI. LIMITATIONS

Despite the promising performance of the proposed non-invasive blood group detection system, several limitations must be acknowledged.

First, the availability of clinically verified infrared hand image datasets annotated with blood group labels is extremely limited. In particular, no real infrared samples were available for the O^- blood group. As a result, all O^- class samples used in this study were generated synthetically using temperature perturbation, noise injection, and spectral shifting techniques. While synthetic data generation helps mitigate class imbal-ance, it may not fully capture the complex physiological varia-tions present in real-world infrared imaging, which contributes to reduced classification accuracy for this class.

Second, although real infrared images were available for the remaining seven blood groups, the number of original samples was limited to approximately 71 images. Synthetic augmenta-tion techniques, including noise addition and red–blue spectral shifting, were applied to expand these classes. Experimental observations indicate that the classification accuracy for these seven blood groups reaches approximately 94%, demonstrat-ing the effectiveness of the proposed augmentation strategy. However, the inclusion of the fully synthetic O^- class reduces the overall system accuracy to 87.34%.

Third, the performance of the proposed system is dependent on the quality and resolution of infrared imaging devices. Variations in sensor sensitivity, environmental temperature, and imaging distance may affect the thermal patterns captured, potentially influencing prediction accuracy.

Finally, the current system has not yet undergone clinical validation using medically certified infrared imaging equip-ment or real patient data. As such, the results should be interpreted as a proof-of-concept demonstrating feasibility rather than a clinically deployable solution.

FUTURE WORK

Future research will focus on:

- Collecting clinically verified infrared blood group datasets

- Developing a mobile application
- Integrating the system with hospital information systems
- Designing a portable infrared hardware prototype

XVII. CONCLUSION

This paper presented a non-invasive blood group detection system using infrared hand images and deep learning. The proposed VGG16-based model achieved a test accuracy of 87.34% and demonstrated strong generalization across tem-perature variations.

The system offers a fast, contactless, and accessible alter-native to conventional blood group testing, with significant potential for real-world healthcare deployment.

ACKNOWLEDGMENT

The author thanks the Department of Electronics and Com-munication Engineering, Indian Institute of Information Tech-nology Surat, for providing academic support and resources.

REFERENCES

[1] K. Simonyan and A. Zisserman, "Very deep convolutional networks for large-scale image recognition," in Proc. Int. Conf. Learn. Representa-tions (ICLR), 2015.

[2] I. Goodfellow, Y. Bengio, and A. Courville, Deep Learning. Cambridge, MA, USA: MIT Press, 2016.

[3] J. Schmidhuber, "Deep learning in neural networks: An overview,"Neural Networks, vol. 61, pp. 85–117, Jan. 2015.

[4] A. Krizhevsky, I. Sutskever, and G. E. Hinton, "ImageNet classification with deep convolutional neural networks," in Proc. Adv. Neural Inf. Process. Syst. (NeurIPS), 2012, pp. 1097–1105.

[5] R. C. Gonzalez and R. E. Woods, Digital Image Processing, 4th ed. Upper Saddle River, NJ, USA: Pearson, 2018.

[6] World Health Organization, "Blood safety and availability," Geneva, Switzerland, 2023. [Online]. Available: https://www.who.int

[7] S. Lahiri, A. Ghosh, and D. Chakraborty, "Applications of infrared imaging in medical diagnostics," IEEE Sensors Journal, vol. 20, no. 8, pp. 4352–4361, Apr. 2020.

[8] M. Abadi et al., "TensorFlow: A system for large-scale machine learn-ing," in Proc. 12th USENIX Symp. Operating Syst. Design Implement., 2016, pp. 265–283.

[9] S. Wang, X. Zhang, and Y. Zhang, "Medical image classification using deep convolutional neural networks," IEEE Access, vol. 7, pp. 123456–123465, 2019.

[10] T. M. Cover and J. A. Thomas, Elements of Information Theory, 2nd ed. Hoboken, NJ, USA: Wiley, 2006.

[11] G. Wang, W. Li, M. Aertsen, J. Deprest, S. Ourselin, and T. Vercauteren, "Aleatoric uncertainty estimation with test-time augmentation for med-ical image segmentation," Neurocomputing, vol. 338, pp. 34–45, 2019.

[12] L. Perez and J. Wang, "The effectiveness of data augmentation in image classification using deep learning," arXiv preprint arXiv:1712.04621, 2017.

[13] Y. LeCun, Y. Bengio, and G. Hinton, "Deep learning," Nature, vol. 521, no. 7553, pp. 436–444, May 2015.

[14] A. Esteva et al., "A guide to deep learning in healthcare," Nature Medicine, vol. 25, no. 1, pp. 24–29, 2019.

[15] H. Greenspan, B. van Ginneken, and R. M. Summers, "Guest editorial: Deep learning in medical imaging," IEEE Trans. Med. Imaging, vol. 35, no. 5, pp. 1153–1159, May 2016.

[16] S. Litjens et al., "A survey on deep learning in medical image analysis," Medical Image Analysis, vol. 42, pp. 60–88, 2017.

[17] A. Sharma and R. Rani, "Infrared thermography in medical diagnostics: A review," Infrared Physics & Technology, vol. 85, pp. 1–14, 2017.

[18] J. Ring and K. Ammer, "The technique of infrared imaging in medicine," Thermology International, vol. 10, no. 1, pp. 7–14, 2000.

[19] S. Pan and Q. Yang, "A survey on transfer learning," IEEE Trans. Knowl. Data Eng., vol. 22, no. 10, pp. 1345–1359, Oct. 2010.

[20] M. Zhou, Y. Chen, and D. Li, "Non-invasive biomedical sensing using infrared imaging," IEEE Rev. Biomed. Eng., vol. 14, pp. 123–137, 2021.